SEISMIC PERFORMANCE OF RC L-SHAPED CORE STRUCTURAL WALLS

Kazuma INADA[1], Kazuto CHOSA[1], Hisataka SATO[2], Susumu KONO[3] and Fumio WATANABE[4]

[1] *Graduate Student, Dept. of Architecture and Architectural Engineering, Kyoto University*
[2] *Structural engineer, Building Construction Division of Engineering, Asanuma Corporation*
[3] *Associate Professor, Dept. of Architecture and Architectural Engineering, Kyoto University*
[4] *Professor Emeritus, Dept. of Architecture and Architectural Engineering, Kyoto University*
(Email: rc.inada@archi.kyoto-u.ac.jp, rc.kono@archi.kyoto-u.ac.jp)

ABSTRACT :

In recent years, a new type of tall buildings is being constructed. They use reinforced concrete core-walls without supplemental moment resisting frames in the seismic force resisting system. RC core-walls offer advantages of open and flexible architecture. In a core-wall building, resistance to seismic forces is provided by a reinforced concrete core.
Three reinforced concrete specimens (L00A, L45A and L45B) of an L-shaped core-wall was constructed with 1/4.5 scale and statically loaded to study the effect of loading direction and the section configuration on the seismic behavior of the core-wall. L45A and L00A were the equilateral L-shaped walls, and L45B was the inequilateral L-shaped wall. L45A showed the deformation followed the Bernoulli's theorem until R=+0.34%. However, after R=+0.5%, the deformation of concrete under compression progressed faster than the deformation of other region and the Bernoulli's theorem was not satisfied any more at this deformation. A simple fiber model well simulated the lateral load - drift angle relation if the moment – curvature relation at the wall base region was properly modeled by considering pull-out of longitudinal reinforcement and local crushing of concrete. However, the analysis did not simulate the load – drift angle relation after R=+0.5%. It is because that the Bernoulli's theorem was not satisfied after R=+0.5% since the local crushing of the concrete took place. Hence, the numerical model based on Bernoulli's theorem was stiffer after R=+0.5%.

KEYWORDS: L-shaped section, core-wall, axial load variation, high-rise RC building

1. INTRODUCTION

In recent years, a new type of tall buildings is being constructed. They use reinforced concrete core-walls without supplemental moment resisting frames in the seismic force resisting system. RC core-walls offer advantages of open and flexible architecture. By eliminating the need for moment resisting frames, smaller framing members or flat slabs can be used for the building floors, and the framing depth of floors can be reduced. In a core-wall building, resistance to seismic forces is provided by a reinforced concrete core that surrounds the elevator banks. A core-wall building eventually realizes lower costs and faster construction (Maffei and Yuen, 2007).

Research on a core-wall has been conducted for last two decades (Hulia et al. 1991, Kumagai et al. 2005, Funaki et al. 2007). Konishi et al. [5] reported that the confinement of concrete at the corner or the end of the section increased the deformation capability and a fiber model assuming Bournoulli's theory (plane section remains plane) simulated the load-displacement relation with good accuracy. Suzuki et al. [6] proposed a method to determine the amount of shear reinforcement for confining purposes based on Konishi's work. However, Nakachi [7] reported that the Bournoulli's theory cannot be applied to a core-wall after the formation of flexure-shear cracks.

Hence, a behavior of core-walls was studied using three 1/4.5 scaled L-shaped core-wall specimens. The specimens were relatively large compared to the existing experimental works and the vertical load up to 12MN was applied to simulate the variation of the vertical loading condition of a multiple core-wall system in practice.

The damage process was recorded and the load-displacement relation was simulated with a fiber model.

2. TEST SETUPS

2.1. Specimens

Figure 1 shows configuration and reinforcement arrangement of three specimens (L00A, L45A and L45B). They were L-shaped core-walls with 1/4.5 scale, and represented the lower three stories in a 40-story reinforced concrete core wall. All wall panels had same thickness of 200mm and height of 2480mm. In this study, the end and corner regions (200mm×200mm) of specimens were confined with shear reinforcement. L45A and L00A were the equilateral L-shaped walls, and L45B was the inequilateral L-shaped wall. Table1 shows mechanical properties of materials. The average strength of concrete was 80 MPa. Steel types were D13 for the vertical reinforcement, D10 for the horizontal reinforcement in unconfined regions and D6 for the hoop reinforcement in confined regions.

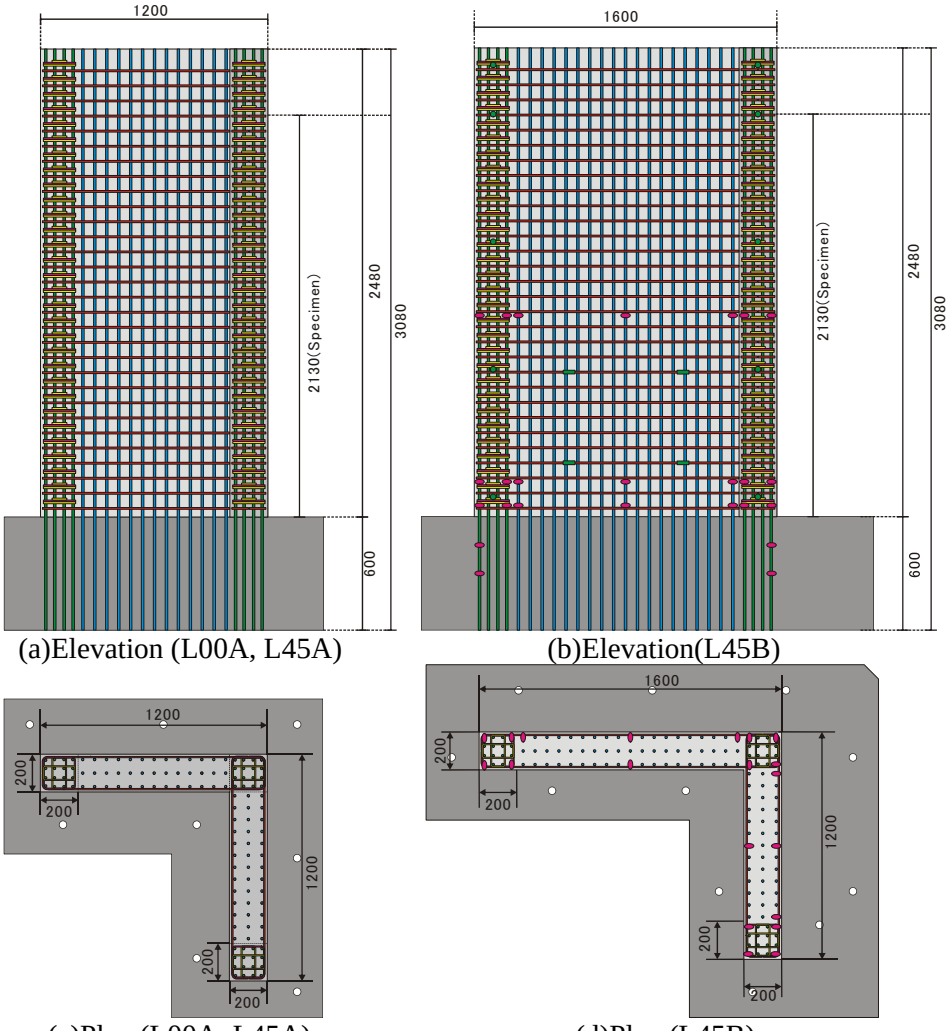

(a)Elevation (L00A, L45A) (b)Elevation(L45B)

(c)Plan (L00A, L45A) (d)Plan (L45B)

Figure 1 Configuration and reinforcement arrangement (Unit: mm)

Table 1 Mechanical properties of materials

(a) Concrete

Specimen	Compressive strength (MPa)	Young's modulus (GPa)	Tensile strength (MPa)
L00A	88.6	39.1	6.35
L45A	76.4	40.4	5.00
L45B	89.1	39.6	5.56

(b)Reinforcement

Type	Yield strength (MPa)	Tensile strength (MPa)	Young's modulus (GPa)
D13	444	611	187
D10	443	607	180
D6	425	539	198

Table 2 Types of reinforcement

Member (Section size)	Bar type		Steel ratio
Column (200×200mm)	Longitudinal	16-D13	5.07%
	Transverse	4-D6 @ 80	0.79%
Wall (Thickness 200mm)	Vertical	3-D13 @ 63	3.02%
	Horizontal	D10 @ 80	0.89%

2.2. Loading System

Figure 2 shows the loading system. In addition to the 3MN hydraulic jack for the lateral load, four hydraulic jacks were used to control the vertical load and three hydraulic jacks were used to control the out-of-plane displacement. Loading protocol of lateral force is shown in Figure 3. The drift is defined as the lateral displacement of the centroid of the section at 2130mm above the upper surface of the stub and the drift angle can be obtained by dividing the drift by 2130mm. Four vertical hydraulic jacks were adjusted so that the height of contraflexure point remained a constant value of 4260mm above the upper surface of the stub. In addition, the long term vertical force was set 0.21Agf'c for L00A and 0.175Agf'c for L45A and L45B, and the axial force was varied as shown in Figure 4. Loading direction differed for each specimen as shown in Figure 5.

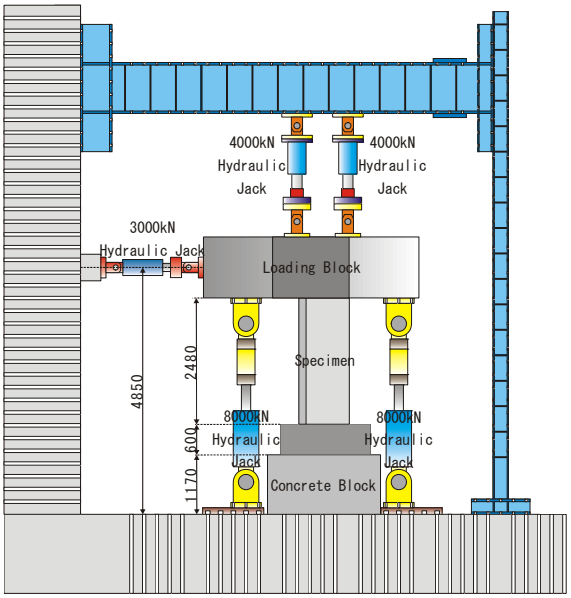

(a)Elevation

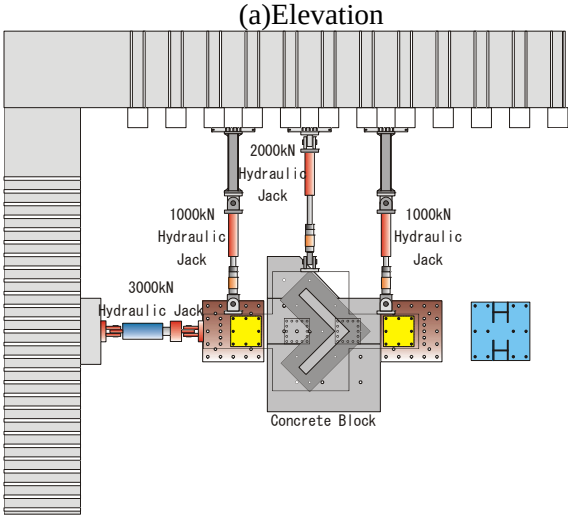

(b)Plan

Figure 2 Loading system (Unit: mm)

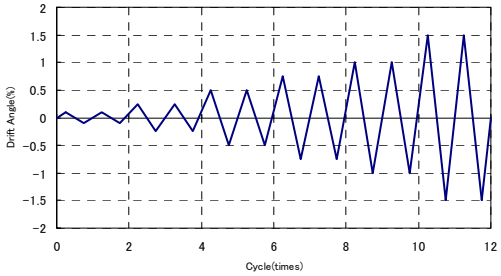

Figure 3 Loading protocol

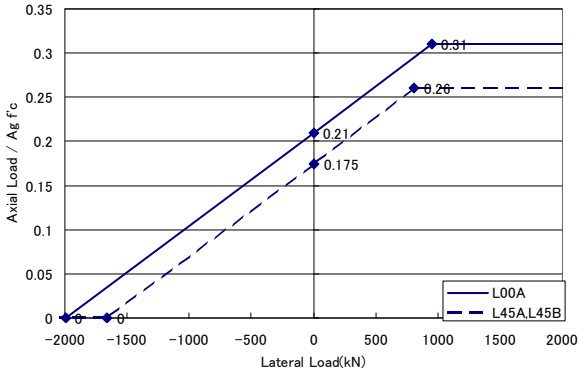

Figure 4 Loading path on axial load ratio - lateral load relation

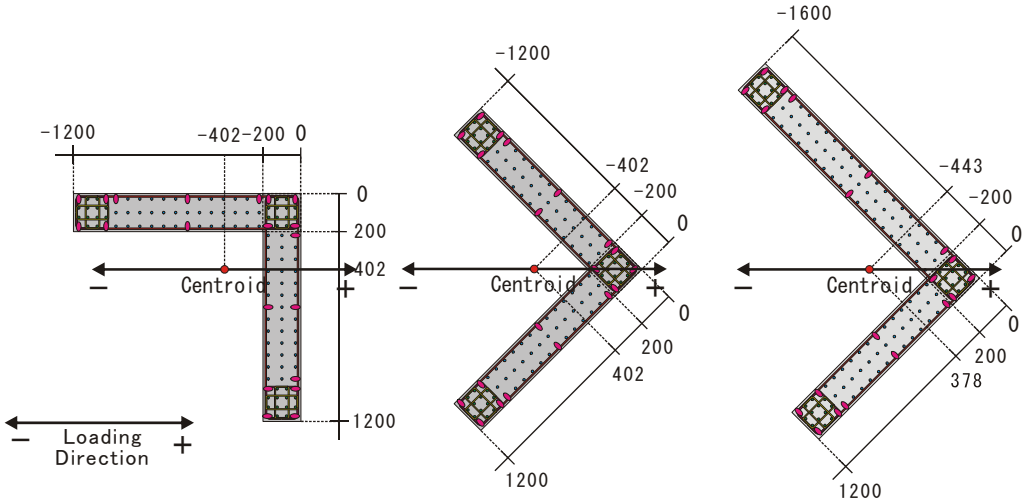

(a)L00A (b)L45A (c)L45B

Figure 5 Loading direction (Unit: mm)

3. TEST RESULTS

3.1. Load-Drift relations

Figure 6 shows the load – drift angle relations and pictures of the specimens after the loading. L00A had the initial flexural cracks at R=+0.1%. Longitudinal reinforcement in the confined region yielded under compression at R=+0.25% and under tension at R=+0.5%. Concrete under compression showed no damage until R=+1.0%. The peak load was reached at R=+1.0% and then the damage of concrete under compression progressed rapidly. The final failure occurred at the base of the wall perpendicular to the loading direction when the concrete failed in shear suddenly. In negative loading, the damage progress was similar to that in positive loading until R=-0.5%. However, the crushing of concrete at section end happened at R=-0.5% earlier than that in positive loading, because a large amount of tensile reinforcement, which mainly was located in the wall perpendicular to the loading direction, carried large tensile force and the compression force of concrete was not able to balance the magnitude.

L45A had the initial flexural cracks at R=+0.16%. Longitudinal reinforcement in the confined region at the corner yielded under compression at R=+0.34%, and the concrete started to crush at R=+0.5%. The peak load was reached at R=1.5% but the deformation progressed without losing too much load carrying capacity until R=2.5%. The final failure occurred at R=2.5% when the concrete at unconfined region crushed under compression. In the negative loading, the initial flexural cracks were found at R=-0.34%, the reinforcement in two confined regions at section ends yielded in compression and that in one confined region at the corner yielded in tension at R=-0.5%. The crushing of concrete at section ends happened at R=-1.5%. The damage under negative direction was less severe than that under positive direction at the same drift ratio because the axial load is lower on the negative side. When the loading was reversed at R=+2.5% to the negative direction, the shear sliding failure occurred near the base of the wall.

L45B showed a similar damage progress to L45A until the positive peak load. The peak load was reached at R=+1.0%. The load carrying capacity degraded gradually till the concrete crushed at R=+1.5%. In the negative loading, the shorter side suffers more severe damage than the longer side.

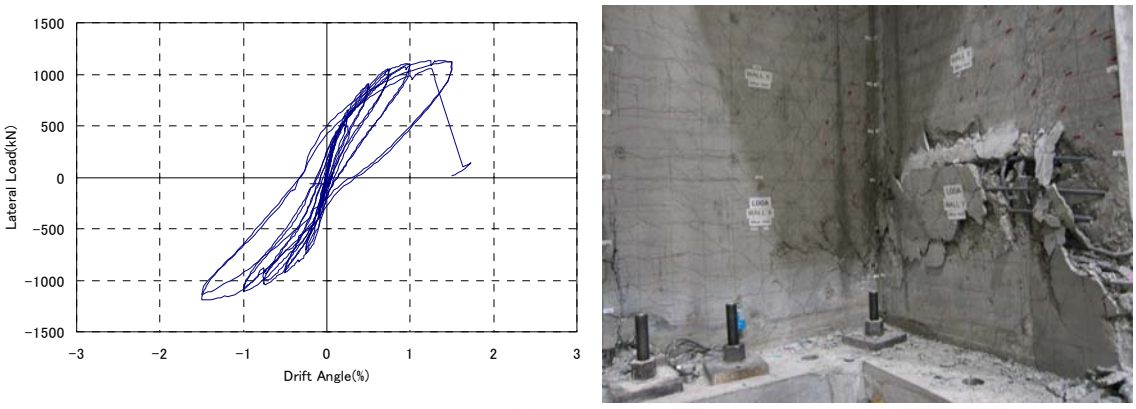

(a)L00A

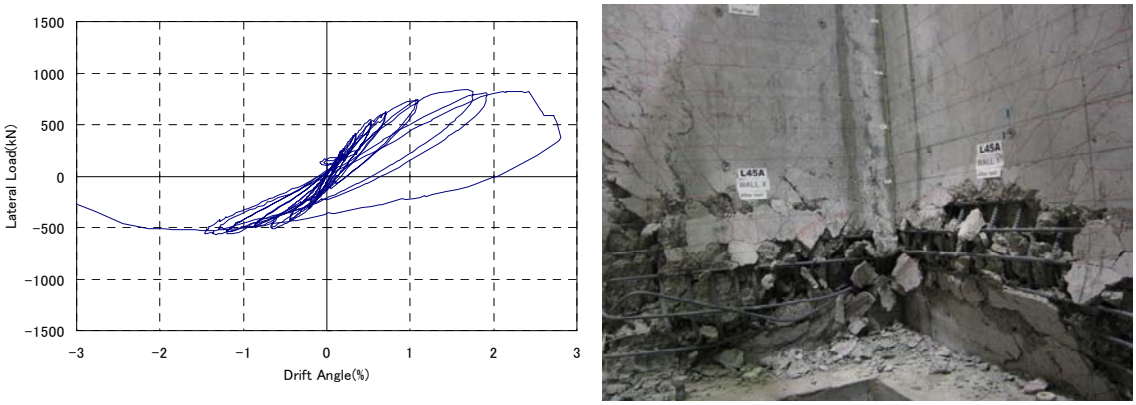

(b)L45A

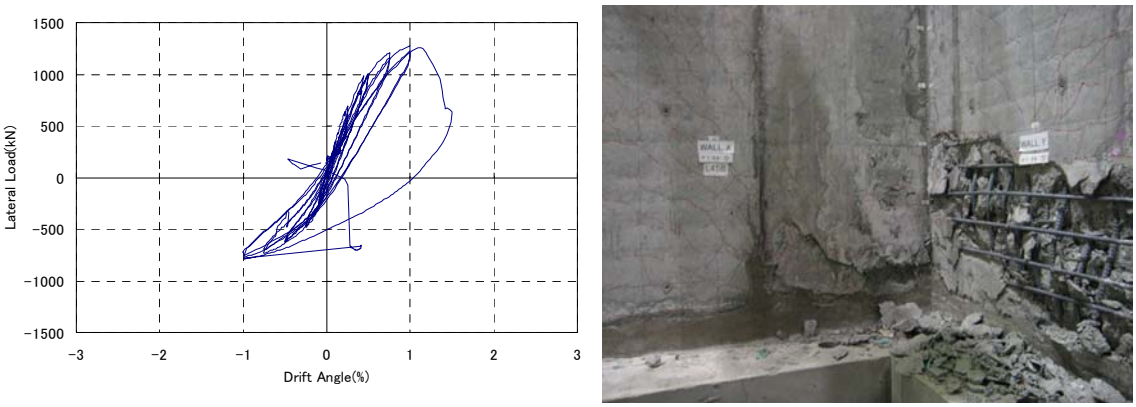

(c)L45B

Figure 6 Lateral load – drift angle relations
and pictures of the specimens after the loading

3.2. Strain-distributions

Strain distributions of the vertical reinforcement in L45A are shown in Figure 7 along the section 60mm above the wall base. The x-axis represents the location of the strain gage. The origin is located at the tip of the corner and sign of the distance is negative for the left wall and positive for the right wall as shown in Figure 5

For drift angles less than R=+0.34%, the strain distribution is nearly linear. However, when the drift angle exceeded R=+0.5%, the strain under compression progressed rapidly and the strain distribution was not linear anymore. In negative loading, the strain distribution is nearly linear until the end of the loading. Two other specimens show similar distributions.

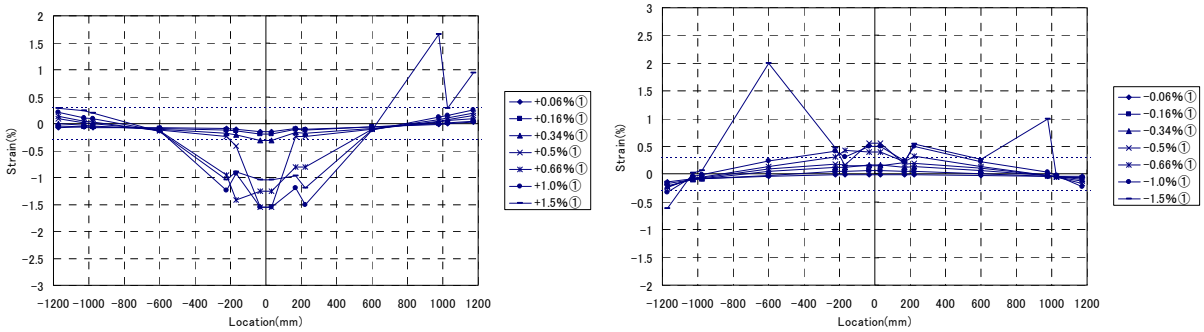

(a)Positive direction (b)Negative direction

Figure 7 Strain distributions in L45A (H=60mm)

4. NUMERICAL SIMULATION

The numerical simulation of a core-wall with a fiber model was conducted by Konishi et al. (1997) and Kumagai et al. (2005) and their procedure was successfully applied to the small scale specimens. A similar procedure was taken to simulate the behavior of L45A. The specimen was divided into 8 layers vertically and each layer was subdivided into 704 fibers as shown in Figure 8. The fictitious fibers above the real specimen were added to achieve a simpler loading conditions and this extended region was assumed rigid. Rigid beams were inserted at the either end of each layer so that the Bernoulli's theorem (plane section remains plane) is satisfied at the layer's boundary. Fibers were categorized into three material groups; plain concrete, confined concrete and longitudinal steel. Hoshikuma's model [9] was slightly modified for plain concrete, Sun and Sakino's model [8] for confined concrete and the elastic-perfectly plastic model for longitudinal steel. The vertical and horizontal loads were proportionally applied to the centroid of the section at the height of the contraflexure point (4260 mm) as indicated in Figure 8.

The lateral load – drift angle relation from the analysis is compared with experimental result in Figure 9. It is clear that the analytical result was too stiff. So the moment – the average curvature relation at each layer was computed and compared with the experimental result in Figure 10. It was found that the difference between the analysis and the experiment was very large at the lowest region of Region Z0 (H=0-105 mm) as shown in Figure 10(a) but the difference in upper region was not very large as can be represented by Region Z1 (H=105-780 mm) in Figure 10(b). This was attributed to the fact that the fiber model does not correctly model the addition a rotation of the wall due to debonding of the vertical reinforcement and crushing of the concrete. Hence, fictitious springs were inserted under the wall so that the moment – curvature relation at Region Z0 was simulated properly. With these fictitious springs, the analytical load – drift angle relation became much closer to the experimental result in Figure 9. However, the analysis still did not simulate the load – drift angle relation after R=+0.5%. As was observed in Figure 7, the Bernoulli's theorem was not satisfied after R=+0.5% since the local crushing of the concrete took place. Hence, the numerical model based on the Bernoulli's theorem was stiffer after R=+0.5% to simulate the real behavior.

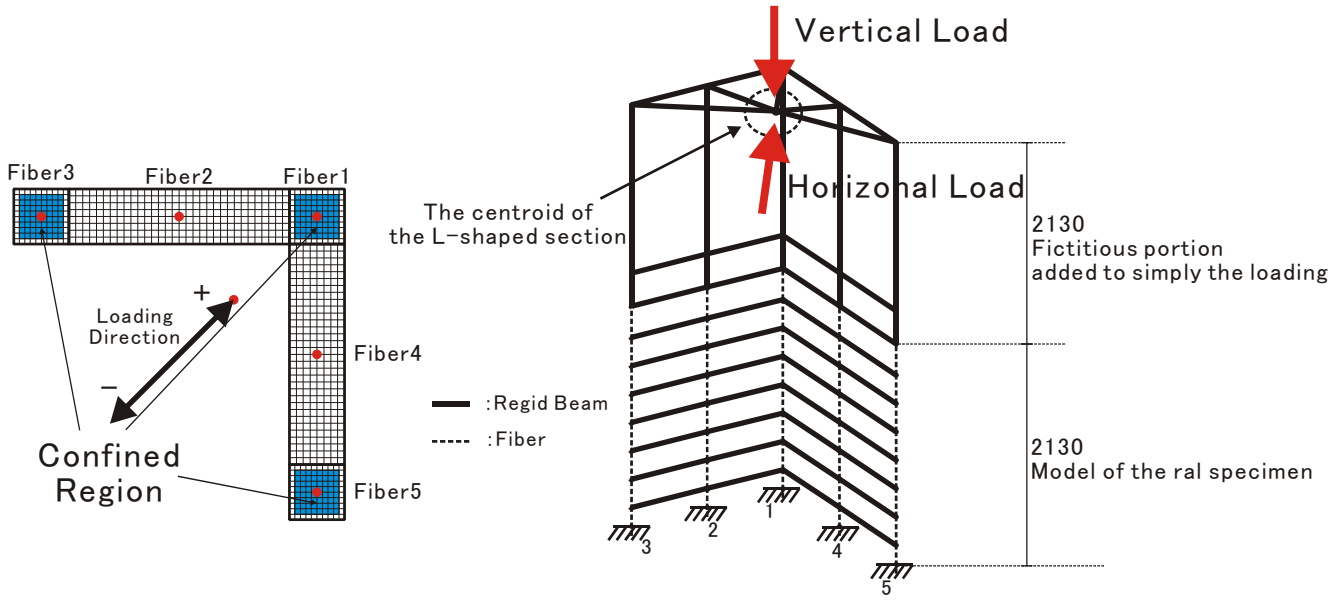

Figure 8 The numerical model (Unit: mm)

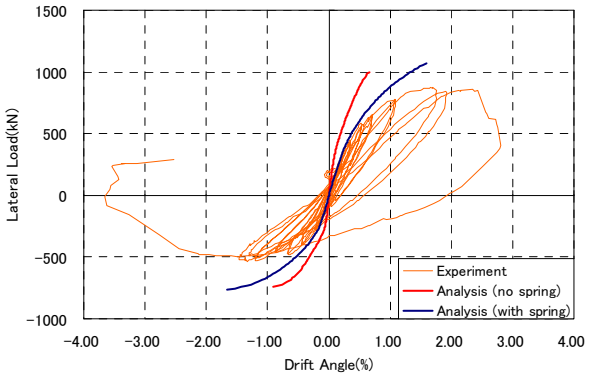

Figure 9 Lateral load – drift angle relation (L45A)

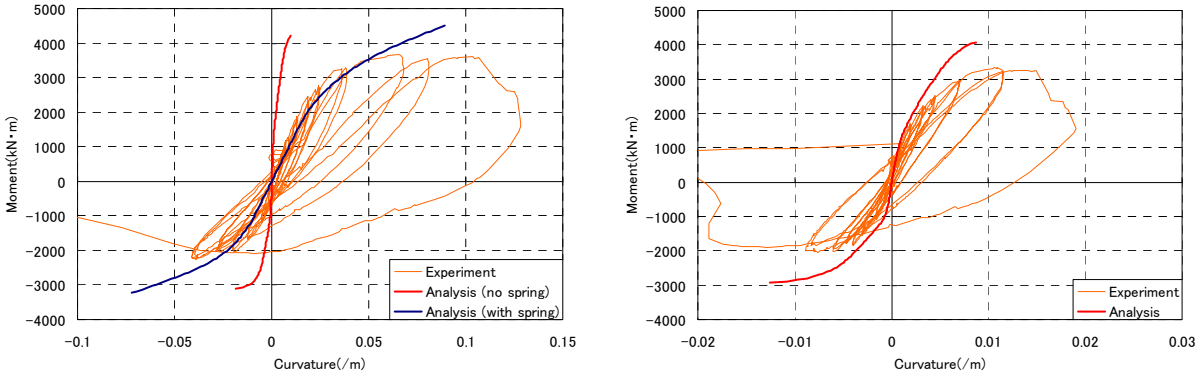

(a)Region Z0 (b)Region Z1

(Analyses with and without spring are identical)

Figure 10 Moment – average curvature relation

5. CONCLUSIONS

Three reinforced concrete models of an L-shaped core-wall was constructed with 1/4.5 scale and statically loaded to study the effect of loading direction and the section configuration on the seismic behavior of the core-wall.

- Three specimens showed large deformation capability until the peak load. The peak load was reached at drift angle around 1.0% in positive direction when experiencing a vertical load about 30% of the axial load capacity. The failure was caused by the crushing of concrete at the compression zone. The failed region in L45A and L45B covered a relatively larger area than predicted by a section analysis and that of L00A covered the whole flange section. It would be better to provide higher confinement to the larger region of concrete to secure high ductility. The peak load was not reached in the negative direction since the axial load was low.

- The deformation followed the Bernoulli's theorem until R=+0.34%. However, after R=+0.5%, the deformation of concrete under compression progressed faster than the deformation of other region and the Bernoulli's theorem was not satisfied any more at this deformation.

- A simple fiber model well simulated the lateral load - drift angle relation if the moment – curvature relation at the wall base region was properly modeled by considering pull-out of longitudinal reinforcement and local crushing of concrete.

ACKNOWLEDGMENTS

This research was conducted as the collaborative research project between Asanuma Corporation(PI: N. Fukumoto) and Kyoto Univ. (PI: S. Kono). The authors appreciate N. Fukumoto, S. Inoue, T. Nakasawa and Y. Tobita for their great contributions to the experimental and analytical work.

REFERENCES

[1] Maffei, J. and Yuen, N. (2007). Seisimic Performance and Design Requirements for High-Rise Building. *Structure Magazine* , April: 28-32.

[2] Huria, V. et al. (1991). 3-D Characterristics of RC Wall Response. *Journal of Structural Engineering* **117:10,** 3149-3167.

[3] Kumagai, H. et al. (2005). Study on 3-dimensional RC Structural Wall Under Flexural Compression (in Japanise). *Journal of Japan Concrete Institute* **16:3,** 59-68.

[4] Funaki, H. et al. (2007). Experimental Study on Structural Performance of RC Shear Walls with L Shaped Section (in Japanise). *Journal of Architectural Institute of Japan* ,699-704.

[5] Konishi, S. et al. (1997). Experimental Study on RC L-shaped Core Structural Wall (in Japanise). *Journal of Japan Concrete Institute* **19:2,** 1083-1088.

[6] Suzuki, N. (1997). A Method to Design Ductile 3-dimensional Reinforced Concrete Shear Walls (in Japanese). *Journal of Architectural Institute of Japan* ,197-198.

[7] Nakachi, T. (2007). FEM Analysis of Reinforced Concrete Core Walls. *Journal of Japan Concrete Institute* **19:3,** 319-324.

[8] Hoshikuma, J., Kawashima, K., Nagaya, K. and Taylor, A. W. (1997). Stress-Strain Model for Confined Reinforced Concrete in Bridge Piers. *Journal of Struct. Engng, ASCE* **123:5,** 624-633.

[9] Sun, Y. and Sakino, K. (1993). Experimental Study on improvement of ductility of RC columns wish high performance Materials (in Japanese). *Journal of Japan Concrete Institute* **15:2,** 719-724.